Journal of Colloid and Interface Science 678 (2025) 595–607

Contents lists available at ScienceDirect

Journal of Colloid And Interface Science

journal homepage: www.elsevier.com/locate/jcis

Regular Article

# Transitioning the production of lipidic mesophase-based delivery systems from lab-scale to robust industrial manufacturing following a risk-based quality by design approach augmented by artificial intelligence

Rafaela Gazzi [a], Rita Gelli [b], Remo Eugster [a], Claudia Bühr [a], Stefan Schürch [a], Raffaele Mezzenga [c], Paola Luciani [a], Simone Aleandri [a,*]

[a] Department of Chemistry, Biochemistry and Pharmaceutical Sciences, University of Bern, Bern, Switzerland
[b] Department of Chemistry "Ugo Schiff" & CSGI, University of Florence, Florence, Italy
[c] Department for Health Sciences and Technology, D-HEST, ETH Zurich, Switzerland

## GRAPHICAL ABSTRACT

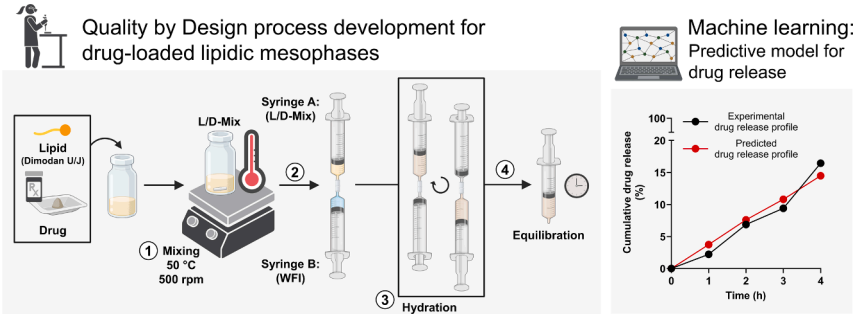


## ARTICLE INFO

*Keywords:*
Lipidic mesophases
Lipid based delivery system
Production method
Quality by design approach
Artificial intelligence

## ABSTRACT

Lipidic mesophase drug carriers have demonstrated the capacity to host and effectively deliver a wide range of active pharmaceutical ingredients, yet they have not been as extensively commercialized as other lipid-based products, such as liposomal delivery systems. Indeed, scientists are primarily focused on investigating the physics of these systems, especially in biological environments. Meanwhile, the production methods remain less advanced, and researchers are still uncertain about how the manufacturing process might affect the quality of formulations. Bringing these products to the market will require an industrial translation process. In this scenario, we have developed a robust strategy to produce lipidic mesophase-based drug delivery systems using a dual-syringe setup. We identified four critical process parameters in the newly developed method (dual-syringe method), in comparison to eight in the standard production method (gold standard), and we defined their optimal limits following a Quality by Design approach. The robustness and versatility of the proposed method were assessed experimentally by incorporating drugs with diverse physicochemical properties and augmented by

* Corresponding author.
*E-mail address:* simone.aleandri@unibe.ch (S. Aleandri).

https://doi.org/10.1016/j.jcis.2024.09.099
Received 20 June 2024; Received in revised form 9 September 2024; Accepted 10 September 2024
Available online 12 September 2024

machine learning which, by predicting the drug release from lipidic mesophases, reduces the formulation development time and costs.

## 1. Introduction

The translation of drug delivery systems from the lab to clinical and commercial scales remains a persisting challenge. Such a transition relies on the scalability of the production method, batch-to-batch reproducibility, and overall cost-effectiveness when compared to current therapies [1]. High complexity of the delivery system and the manufacturing process might also contribute to the delay in the progress of formulations developed in academic settings. In this scenario, it becomes crucial to establish reproducible and robust methods during the early stages of drug formulation development. The identification and correct management of all sources of variability affecting a process are ensured by a systematic and risk-based Quality by Design approach (QbD) [2], encouraged by Food and Drug Administration (FDA) and the European Medicine Agency (EMA) [3,4].

Lipidic mesophases (LMP) are promising controlled drug delivery

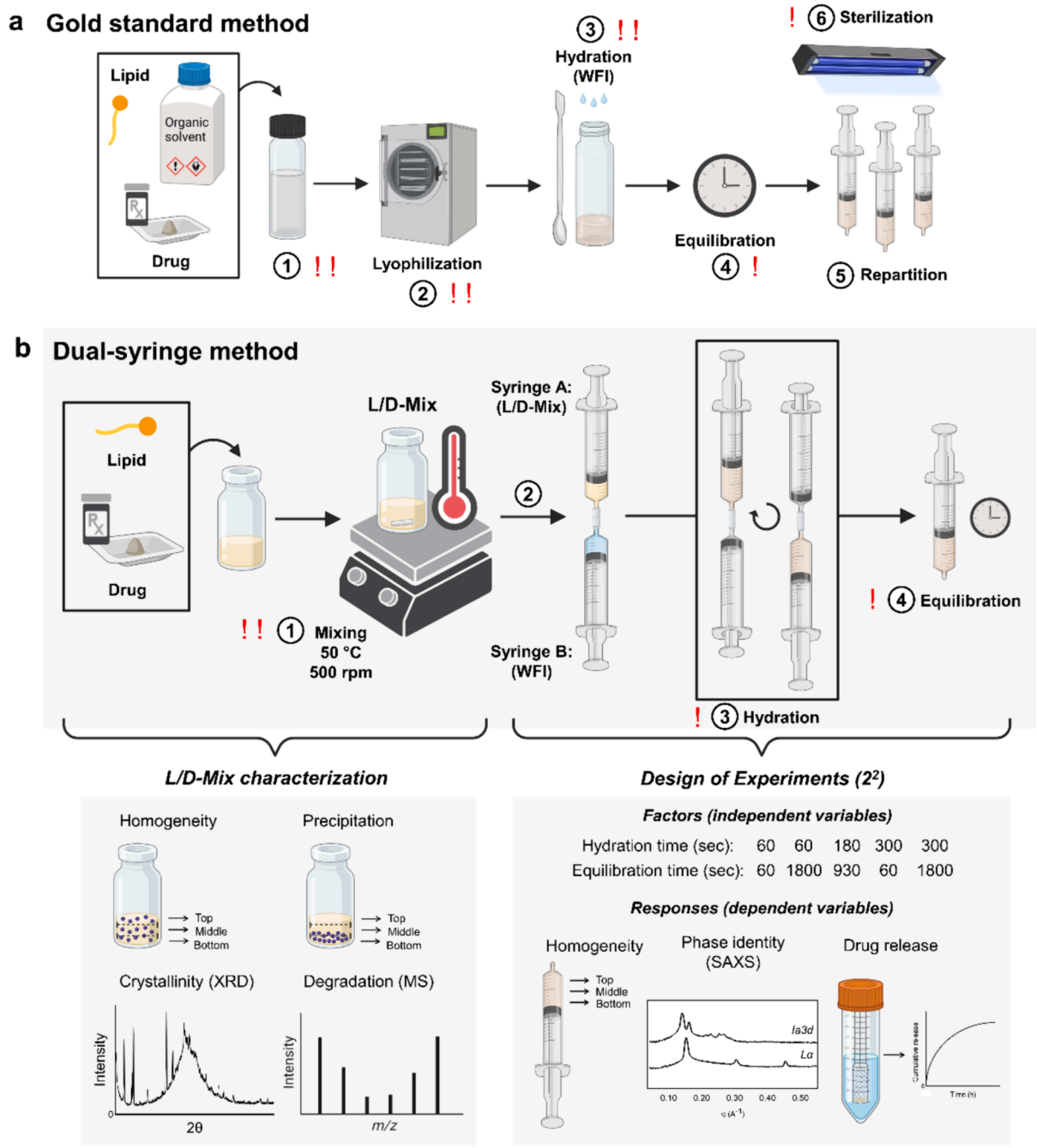


**Fig. 1.** Process flow charts for LMP-based drug delivery systems production by (a) gold standard method and (b) dual-syringe method. The numbers in panels a and b represent the steps of the production method, and each red exclamation point represents one critical process parameter (CPP) or critical material attribute (CMA). WFI: water for injections. (For interpretation of the references to colour in this figure legend, the reader is referred to the web version of this article.)

systems, yet far less explored than lipid-based nanoparticles. They are formed by the self-assembly of amphiphilic lipids in aqueous solutions and allow the incorporation and release of molecules with various polarities and sizes [5–15]. The nature of the lipid, water content and temperature influence the lipid arrangements, which range from the less viscous (and pseudoplastic) lamellar to the more structured (and viscoelastic) inverse bicontinuous cubic phase [16]. Although the latter has an optimal rheology to act as a drug depot for a broad range of applications [5,6,17,18], its high viscosity makes the administration challenging. Water can overcome this challenge by triggering the in situ formation of gelled lipidic structures, starting from a liquid or less viscous material. For instance, low viscous lamellar phases, which absorb water and transform into a structured gel in-situ, have been reported for subcutaneous injection [7,18]. In the pharmaceutical industry scenario, the Swedish company Camurus developed the FluidCrystal® technology, which is characterized by an ethanolic solution containing lipids and drug that transforms into LMP-based gel upon contact with water [19,20].

Our research group recently developed an LMP-based temperature-triggered in situ forming gel (TIF-Gel) for the topical treatment of ulcerative colitis [17], where temperature was selected as a gelation trigger instead of water, since the volume and composition of the fluid in the rectum are affected by physiological or pathological conditions [21,22]. Despite our encouraging results, the formulation was manufactured in a small-scale setup following a well-established procedure (named here as gold standard), but its scalability is limited by the use of organic solvents, lyophilization step, long equilibration times, sterilization of the final gel-like formulation, among other factors (see Fig. 1a). Unfortunately, there is limited information available on the large-scale production of LMP-based drug delivery systems as most research has been focused on the physicochemical characterization of these materials [19,23]. Moreover, academia extensively employs the conventional method of quality by testing, in which the quality of the end-product of each batch is assessed based on predefined specifications [24]. In case of quality deviations, the batch is discarded, and it is difficult to identify and understand the root cause of failure [24,25].

In contrast, here we employed a QbD approach to develop an alternative production method for LMP-based drug delivery systems. Our strategy is based on a dual-syringe setup (see Fig. 1b) inspired by an already published protocol in which microliter syringes have been employed to produce mesophases intended for the crystallization of membrane proteins [26]. Nevertheless, differently from this method, our manufacturing procedure precisely defines the optimal limits for the identified high-risk variables and, therefore, establishes a controlled process. The versatility of the dual-syringe method to produce LMP-based drug delivery systems was experimentally assessed by the incorporation of drugs with diverse physicochemical properties. Machine learning has demonstrated its utility in data-driven formulation development, aiding in the prediction of critical quality attributes (such as drug release) and guiding the selection of optimal process parameters, consequently reducing both the time and costs associated with drug formulation development. Among the numerous advantages of our approach, we emphasize the avoidance of organic solvents, lyophilization step and sterilization of the final gel, as well as the mesophase equilibration within one minute. The method was developed taking into consideration also other aspects, such as the packaging of the pharmaceutical product, its storage, and patient compliance.

## 2. Experimental section

### 2.1. Materials

Dimodan U/J was donated from Danisco (Denmark). This industrial food grade quality analogue of monolinolein is composed of a mixture of monoglyceride derived from oleic fatty acid with a minimum monoglycerides content of 90 %. Pure monolinolein (MLO, >99 %) was purchased from NU-Check Prep, Inc. (MN, USA). Tofacitinib citrate (TOFA, >99 %) was obtained from LC laboratories (Woburn, MA), tacrolimus (TAC, 99.3 %) was obtained from R&S Pharmchem Co., Ltd (Shanghai, China), 5-aminosalicylic acid (5-ASA, 99.9 %) was obtained from Sigma-Aldrich Chemie GmbH (Taufkirchen, Germany), budesonide (BUD, 97 %) was obtained from Thermo Scientific (Fair Lawn, United States), and cyclosporine A (Cy.A, 98.5 %) was obtained from Abcr GmbH (Karlsruhe, Germany). Ultrapure water (18.2 MΩ.cm) was produced by Barnstead Smart2pure (Thermo Scientific). Analytical grade methanol and acetonitrile were supplied by Fisher Scientific (Schwerte, Germany). Ethanol absolute was supplied by VWR chemicals BDH (London, UK). Dimethyl sulfoxide (≥99.5 %), HEPES salt (≥99.5 %) and Tween® 80 (Ph. Eur. grade) were obtained from Carl Roth GmbH & Co. (Karlsruhe, Germany).

### 2.2. LMP production by the dual-syringe method

The first step of the dual-syringe method consists of producing the L/D-Mix, which is the mixture of lipid (84 % w/w) and drug (TOFA, 5-ASA, BUD, and Cy.A at 5 % w/w, 5 mg/100 mg of LMP, and TAC at 1 % w/w, 1 mg/100 mg of LMP). The molten lipid (Dimodan U/J) and the appropriate amount of drug were weighed into 10 mL glass vials and mixed in a magnetic stirrer at 500 rpm and 50 °C for 15 min. In the second step, 500 mg of L/D-Mix was transferred to a 1 mL syringe (Fisher Scientific, Pittsburgh, US), named syringe A, and a second syringe, named syringe B, was filled with water for injections (WFI, 16 % w/w). Both syringes were attached with a syringe connector (Combifix® Adapter Luer-Lock female/female), and the LMP was hydrated by transferring the content of syringe A to syringe B and vice-versa for a determined time, followed by the equilibration of the gel.

#### 2.2.1. Design of experiments

Optimal hydration and equilibration times for LMP production were determined by a $2^2$ full factorial Design of Experiments (DoE) generated by Minitab® 18.1 software. The factorial design consisted of four factorial points ($2^2$) and one centre point. Therefore, five experiments were performed with TOFA, TAC and 5-ASA. We have selected hydration time, ranging from 60 to 300 s, and equilibration time, ranging from 60 to 1800 s, as factors (i.e., independent variables). As responses (i.e., dependent variables), drug homogeneity within the syringe, LMP phase geometry and 4-h drug release were used. The experimental runs (n = 2) are shown in Table 1. To validate the derived model, BUD and Cy.A were used to produce LMP applying the optimal hydration and equilibration times (n = 2).

### 2.3. LMP production by the gold standard method

As a comparison to the dual-syringe method, LMP were also prepared as previously described [17]. Shortly, lipid (MLO) and drug (in the same concentrations used previously) were dissolved in organic solvent, which was completely removed under reduced pressure (freeze-drying for 24 h at 0.22 mbar). After that, a weighed amount of water was added to the dried lipid/drug, and mixed and centrifuged (10 min, 5000 g), alternatively, at room temperature until a homogeneous gel was obtained. The LMP were equilibrated for 48 h at room temperature and in the dark before analysis.

**Table 1**
DoE experimental runs.

| Experimental runs | Mixing time (s) | Equilibration time (s) |
|---|---|---|
| 1 | 60 | 60 |
| 2 | 60 | 1800 |
| 3 | 180 | 930 |
| 4 | 300 | 60 |
| 5 | 300 | 1800 |

### 2.4. Drug homogeneity in L/D-Mix and LMP

Drug homogeneity was evaluated in two batch sizes of L/D-Mix (700 mg and 1500 mg) by drug quantification in three sections of the vials (top, middle and bottom) at time-zero (t = 0) and after 2 weeks (t = 2 weeks) at 2–8 °C. L/D-Mix containing TOFA, TAC or 5-ASA were assessed after 5, 10 and 15 min of mixing, whereas drug homogeneity of L/D-Mix containing BUD or Cy.A was determined after the optimal mixing time.

Drug homogeneity in the LMP produced by the dual-syringe method was verified by drug quantification in three sections of the syringe (top, middle and bottom) immediately after the hydration and equilibration times defined by the DoE. TOFA, TAC, BUD and Cy.A concentrations were determined by reversed-phase high-performance liquid chromatography (RP-HPLC) using a Macherey-Nagel Nucleosil 100-5 C18 (4.0 × 250 mm; 5.0 μm particle size) column. Details of the RP-HPLC quantification methods are described in Table 2. Data were collected and analysed using the software Chromeleon 7 (Thermo Fisher). 5-ASA concentration was determined by absorbance using a microplate reader (Spark 10 M, Tecan, Switzerland). The maximal absorbance wavelength of the drug in dimethyl sulfoxide, at 20 °C, was 364 nm, which was used for drug quantification in the L/D-Mix and in the LMP. The maximal absorbance wavelength of the drug in HEPES (20 mM, pH 7.4), at 20 °C, was 332 nm, which was used for drug quantification after the drug release experiments.

### 2.5. X-ray powder diffraction

X-ray powder diffraction (XRPD) was applied to investigate whether Dimodan U/J induced changes in the crystallinity of the drugs. The drugs alone (at t = 0), L/D-Mix in the mixing vial (at t = 0 and t = 2 weeks) and L/D-Mix stored in the syringe (t = 3 months) were analysed on a D8 Advance (Bruker, Milan, Italy). Cu Kα radiation was used as X-ray source (λ = 1.54 Å) operating at voltage of 40 kV and filament current of 40 mA, a 2θ range of 3–50°, a step size of 0.03°, and a time/step of 0.3 s. A thin layer of each sample was spread onto a Si-zero background sample holder and analysed. The crystallinity degree % of the formulations was estimated as the ratio between the area under the crystalline peaks and the area of the whole pattern, after the removal of the background curve [27]. The area under the crystalline peaks was obtained by subtracting the area of the broad amorphous peak at about 20° from the total area under the pattern. The analysis was carried out using the software TOPAS (Bruker).

**Table 2**
HPLC conditions for quantification of TOFA, TAC, BUD and Cy.A. TFA: trifluoroacetic acid.

| Drug | Mobile phase | Flow rate | Injection volume | Column temperature | Wavelength |
|---|---|---|---|---|---|
| TOFA | Acetonitrile: methanol: water (13:13:74 % v/v) + 0.1 % TFA | 1.0 mL/min | 5 μL | 25 °C | 278 nm |
| TAC | Methanol: water (80:20 % v/v) + 0.1 % TFA | 1.0 mL/min | 5 μL | 50 °C | 214 nm |
| BUD | Acetonitrile: water (70:30 % v/v) + 0.1 % TFA | 0.5 mL/min | 15 μL | 40 °C | 254 nm |
| Cy.A | Acetonitrile: water (70:30 % v/v) + 0.1 % TFA | 1.0 mL/min | 10 μL | 80 °C | 220 nm |

### 2.6. Mass spectrometry

Liquid chromatography-mass spectrometry (LC-MS) analyses were performed on a QTrap 5500 mass spectrometer (Sciex, Baden, Switzerland) equipped with an electrospray ion source coupled to an Ultimate 3000 HPLC system (Thermo Fisher Scientific, Reinach, Switzerland). A Reprosil C18, 5 μm, 125 mm × 2 mm (Dr. Maisch, Ammerbuch-Entringen, Germany) HPLC column was used for separation of the drugs. The mobile phase consisted of 10 mM ammonium formate in water (eluent A) and acetonitrile (eluent B). The mobile phase was kept at 5 % eluent B for the first 4 min followed by a gradient up to 95 % eluent B within the next 4 min, which was maintained for another 3 min. All solvents were of LC-MS grade and obtained from Merck (Buchs, Switzerland). TOFA and TAC were analysed in the positive ion mode, and 5-ASA in the negative ion mode.

Quantitation of drugs was performed by multiple reaction monitoring using the following transitions: $[TOFA + H]^+$: *m/z* 312.7/148.9 (quantifier), 312.7/164.8 (qualifier); $[TAC + NH4]^+$: *m/z* 821.6/768.5 (quantifier), 821.6/576.5 (qualifier); $[5\text{-}ASA - H]^-$: *m/z* 151.8/109.7. From the stock solutions of TOFA and TAC (1 mg/mL methanol each), calibration solutions with 5, 10 and 20 μg/mL were prepared and further diluted 1:10 with water prior to analysis in duplicates. The calibration solutions of 5-ASA contained 2.5, 5, 7.5 and 10 μg/mL and were processed accordingly. The L/D-Mix samples were prepared for analysis as follows: 1–2 mg of L/D-Mix and 10 mL of methanol were thoroughly mixed. L/D-Mix containing TOFA and TAC were diluted with water in a ratio of 1:5 prior to analysis, and L/D-Mix containing 5-ASA was diluted with water in a ratio of 1:10. Analyses were performed in triplicates.

### 2.7. Drug release

Drug release from the LMP was evaluated using an experimental setup consisting of a 50 mL tube and a custom-made metallic basket. The formulations were weighed inside the basket which was then placed in tubes containing the release media: HEPES buffer pH 7.4 for TOFA and 5-ASA, HEPES buffer pH 7.4 enriched with 10 % (v/v) ethanol for TAC, aqueous solution with Tween 80 2 % (w/v) for BUD, and HEPES buffer pH 7.4 enriched with 30 % (v/v) ethanol for Cy.A. This setup was placed in a shaking incubator at 37 °C and 100 rpm, and the release medium was collected and completely replaced with fresh buffer every hour, up to 4 h. Aliquots were lyophilized and resuspended in mobile phase, and the drug content was determined.

#### 2.7.1. Predictive model for drug release

A mathematical model for predicting drug release from the LMP produced by the dual-syringe method was developed using KNIME (v. 5.2.2). We integrated molecular descriptors derived from SMILES codes with stratified sampling and cross-validation techniques to predict drug release at four time points (1 h, 2 h, 3 h, 4 h). The dataset containing drug release data was loaded into the program, and molecular descriptors (such as SlogP and Lipinski's Hydrogen bond donors) were extracted using RDKit nodes. Further, formulation parameters such as the hydration and equilibration times were used as features. The data set was stratified and sampled into training and testing sets (80:20) based on the drug variable. A combined parameter optimization and 5-fold cross-validation were performed on an XGBoost regression model, per time point, using the training set to optimize model parameters. The optimized parameters were fed into training a new model which was then tested using the test data set. To assess predictive power, the separate models underwent six resets and runs per time point. Validation of the models involved exposing them to a drug molecule unknown to the model, predicting its release six times, and comparing the predictions to wet lab experiments. The workflow can be accessed publicly here: hub.knime.com/Eugster.

### 2.8. Small angle X-ray scattering

Small angle X-ray scattering (SAXS) was applied to determine the phase identity and symmetry of the LMP. The measurements were performed on a Bruker AXS Micro using a microfocused X-ray source (λ Cu Kα = 1.5418 Å) operating at voltage of 50 kV and filament current of 1000 μA. The diffracted X-ray signals were collected by a 2D Pilatus 100 K detector. The scattering vector was calibrated using silver behenate. Data were collected and azimuthally averaged using the Saxsgui software to yield 1D intensity vs. scattering vector Q, with a Q range from 0.001 to 0.5 $Å^{-1}$. For all measurements, the samples were placed inside a stainless-steel cell between two thin replaceable mica sheets and sealed by an O-ring, with a sample volume of 10 μL and a thickness of ~1 mm. Measurements were performed at 25 °C and 37 °C and the scattered intensity was collected over 10 min.

### 2.9. Confocal Raman microscopy

Confocal Raman experiments were performed using a Renishaw inVia$^{TM}$ Qontor® confocal Raman microscope (Wotton-under-Edge, UK) equipped with a 785 nm laser, a front-illuminated CCD camera, and a research-grade Leica DM 2700 microscope.

The spectra of the single components (Dimodan U/J, TOFA, TAC, BUD, Cy.A) were collected in the range 150–3200 $cm^{-1}$ using a 20x objective (numerical aperture 0.40, working distance 1.15 mm), laser power 100 mW, exposure time of 20 s and 3 accumulations per spectrum. For 5-ASA, due to fluorescence phenomena, the laser power was decreased at 10 mW and the number of accumulations was 5. A polynomial baseline was subtracted from all the spectra, which were then normalized at the respective peak maximum.

The maps were obtained with a 5x objective (numerical aperture 0.12, working distance 14 mm); for each sample, two maps of 1.6 mm × 1.0 mm were collected (step size: 50 μm), imaging a total area of 1.6 mm × 2 mm. The spectra were collected in the 600–1710 $cm^{-1}$ range, with a laser power 100 mW, exposure time 3 s and 2 accumulations (4 in the case of the formulations with 5-ASA). All spectra were processed with cosmic ray removal, baseline subtraction and smoothing. The maps were analysed by reporting the intensity with respect to the baseline of peaks characteristic of the lipid and the drugs, namely for the formulations with TOFA: 1490 $cm^{-1}$ TOFA and 1656 $cm^{-1}$ Dimodan U/J, for the formulations with 5-ASA: 816 $cm^{-1}$ 5-ASA and 1656 $cm^{-1}$ for Dimodan U/J, and for the formulations with BUD: 645 $cm^{-1}$ BUD and 1299 $cm^{-1}$ Dimodan U/J.

### 2.10. Rheology experiments

A stress-controlled rheometer (Modular Compact Rheometer MCR 72 from Anton Paar, Graz, Austria) was used in cone-plate geometry (0.993° angle and 49.942 mm diameter). First, a viscosity vs. shear rate curve was performed at 25 °C for LMP produced by the dual-syringe method (180 s hydration and 60 s equilibration) and by the gold standard method. To investigate whether Dimodan U/J would have an influence on the final viscosity of LMP, MLO was also used to prepare LMP by both methods. After that, amplitude strain sweep was performed at frequency of 1 Hz and strain percentages between 0.002 and 100 % to determine both the linear viscoelastic region and the flow point.

## 3. Results

### 3.1. Production of drug-loaded LMP

Mesophases have the capability to host and release a plethora of molecules. However, despite their potential as drug carriers, a robust and scalable production method has yet to be established. Each research laboratory employs different manufacturing methods, resulting in uncontrollable critical process parameters (CPPs) and, consequently, batch-to-batch variability and a decline in the quality of the pharmaceutical product. Moreover, these laboratory-scale production methods have not been correlated with the ensuing formulation performance, such as drug encapsulation and release. Therefore, a more suitable strategy for producing LMP-based semisolid drug delivery systems, employing QbD, was developed, and the versatility of the proposed method was tested through the incorporation of five drugs. The high-risk variables associated with the process were first identified, and then they were reduced and optimized to establish a robust, reproducible, and scalable process (all details reported in the Supplementary Information, Supplementary Tables 1-5). The process flow charts of LMP production by the gold standard method and the proposed dual-syringe method are illustrated in Fig. 1a and b, respectively. As shown by the numbered steps on Fig. 1a, the gold standard method requires (1) the solubilization of the lipid and the drug in organic solvents followed by (2) lyophilization for removal of the solvent. The mixture of lipid and drug is (3) hydrated and mixed until a homogeneous gel is formed, and (4) equilibrated for several hours. Next, (5) the syringes (or any other primary packaging) are individually filled and (6) a sterilization step might be required. This approach presents numerous critical material attributes (CMAs) and CPPs that could affect the product's quality. For instance, *(I)* proper solubility of lipid and drug in organic solvent, *(II)* stability of the lipid and/or drug in solution, *(III)* complete removal of the organic solvent, *(IV)* stability of the lipid and/or drug after lyophilization, proper *(V)* hydration and *(VI)* equilibration times, *(VII)* drug stability after hydration and *(VIII)* sterilization of the formulation. Here, we have developed an alternative method to produce drug-loaded LMP using TIF-Gel composition (16 % w/w of water) as a starting point. As shown in Fig. 1b, (1) lipid and drug are mixed for a defined time (L/D-Mix), and (2) loaded into the syringe. The (3) hydration and (4) equilibration steps occur directly in the syringe, which is the primary packaging, and only before the application. This new approach presents fewer CPPs that could affect the quality of the final gel. However, important parameters to be controlled are *(I)* proper homogenization of L/D-Mix, *(II)* drug stability in this mixture, and proper *(III)* hydration and *(IV)* equilibration times. Besides optimizing the production method, we have altered the lipid component from MLO to an industrial food grade quality analogue, Dimodan U/J, considering its lower cost and characteristic waxy-solid consistency.

### 3.2. LMP production by the dual-syringe method

#### 3.2.1. Production steps 1 and 2

The first step of the proposed method consists of mixing of the lipid, Dimodan U/J, and the drug at 500 rpm and 50 °C (Fig. 1b, Step 1). TOFA, TAC and 5-ASA were homogeneously distributed in the L/D-Mix after 15 min of mixing (Fig. 2a, top). Also, it was possible to increase the volume of L/D-Mix (from 700 mg to 1500 mg of lipid) and maintain the mixing time without compromising drug homogeneity. Lower mixing times (5 and 10 min) were not sufficient to obtain a uniform drug distribution (Supplementary Fig. S1). Afterwards, the optimal mixing time was validated with budesonide (BUD) and cyclosporine A (Cy.A) using the lipid in the range of 700–1500 mg (Fig. 2a, dashed box). BUD was properly homogenised after 15 min, however Cy.A needed a longer mixing time. Drug aggregates were formed at the beginning of this step and 25 min were needed for a complete dispersion of this drug. After 2 weeks of storage at 2–8 °C, no significant drug precipitation was observed (Fig. 2a, bottom). Whereas the type of crystalline phase was preserved (Fig. 2b), the degree of crystallinity of all formulations slightly increased after storage, as expected (Fig. 2c). Evaluation of drug recovery from L/D-Mix samples after 1-month storage at room temperature and 2–8 °C was performed by quantitative LC-MS using a multiple reaction monitoring approach. Transitions from molecular ions to characteristic fragment ions were chosen for enhanced selectivity. High drug recovery percentages were observed for all drugs analysed at both conditions (Supplementary Fig. S2). Moreover, no changes in the

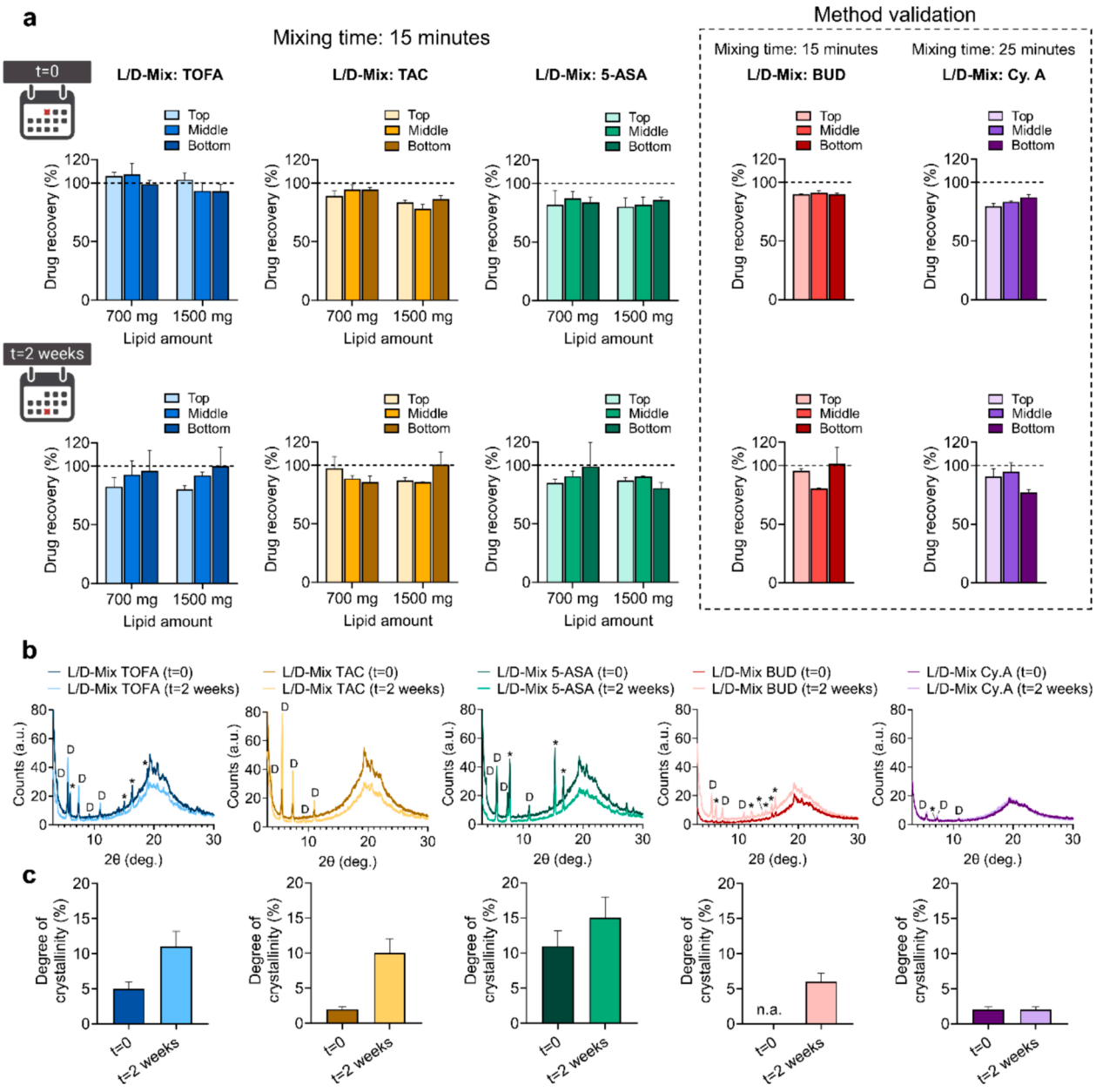


**Fig. 2.** Characterization of L/D-Mix after 15 min of mixing time regarding drug content and XRPD pattern. (a) Drug recovery of TOFA, TAC and 5-ASA from three sections of the L/D-Mix with batch sizes of 700 mg and 1500 mg at t = 0 (top) and t = 2 weeks (bottom). Dashed box: Validation of the mixing method by drug quantification (BUD and Cy.A) in three section of the L/D-Mix. (b) L/D-Mix XRPD pattern, where D represents the reflections of Dimodan U/J, and the asterisk represents the reflections of the drugs; and (c) degree of crystallinity at t = 0 and t = 2 weeks. Results are shown as mean ± SD (n = 2).

crystalline phase were detected after 3-month storage of L/D-Mix in the syringe (Supplementary Fig. S3). The XRPD pattern of pure Dimodan U/J and drug powders are shown in Supplementary Fig. S4.

### 3.2.2. *Production steps 3 and 4*

The steps 3 and 4 correspond to the hydration and equilibration of the LMP. In total, five LMP were produced by the dual-syringe method for each drug group (TOFA, TAC and 5-ASA) using different hydration and equilibration times (factors) defined by DoE (Table 1). We assessed whether these factors influence the drug homogeneity, the drug release profile, and the phase identity of the mesophase. As shown in Fig. 3a, the distribution of the drug within the syringe is not affected by the two factors, as homogeneous LMP were obtained using the minimum hydration/equilibration times (60/60 s). Next, we investigated if both the factors (hydration and equilibration times) and the method used for LMP production affect the drug release. The results were correlated by plotting the ratio between the total amount of drug released from the LMP prepared by the dual-syringe method and the LMP prepared by the gold standard method (Fig. 3b; see also Supplementary Fig. S5). Clearly, the amount of drug released is not affected by the different hydration or equilibration times, given the similar ratio values obtained for each individual drug group. On the other hand, our results suggest that the production method can influence drug release and this phenomenon is drug dependent. Similar amounts of TAC were released from LMP produced either by the dual-syringe method or the gold standard method, resulting in ratio values close to 1 (Fig. 3b, centre), and the LMP containing 5-ASA presented similar behavior (Fig. 3b, right). On the contrary, lower amounts of TOFA were released from LMP prepared by the dual-syringe method, resulting in ratio values lower than 1 (nearing 0.5) (Fig. 3b, left). SAXS measurements were conducted at 25 °C and 37 °C to

**a**

| | | TOFA (5% w/w) MW: 504.50 g/mol Log P: 1.15 | | | | | TAC (1% w/w) MW: 804.02 g/mol Log P: 3.20 | | | | | 5-ASA (5% w/w) MW: 153.13 g/mol Log P: 1.20 | | | | |
|---|---|---|---|---|---|---|---|---|---|---|---|---|---|---|---|---|
| Hydration time/ equilibration time (sec) | | 60/ 60 | 60/ 1800 | 180/ 930 | 300/ 60 | 300/ 1800 | 60/ 60 | 60/ 1800 | 180/ 930 | 300/ 60 | 300/ 1800 | 60/ 60 | 60/ 1800 | 180/ 930 | 300/ 60 | 300/ 1800 |
| Drug % | Top | 6.06 ±0.66 | 5.23 ±0.68 | 5.02 ±0.31 | 4.86 ±0.23 | 5.56 ±0.32 | 1.08 ±0.01 | 1.15 ±0.01 | 1.08 ±0.05 | 1.19 ±0.21 | 1.12 ±0.12 | 4.57 ±0.04 | 4.92 ±0.34 | 4.92 ±0.11 | 4.08 ±0.02 | 4.77 ±0.01 |
| | Middle | 5.70 ±0.31 | 5.55 ±0.72 | 5.53 ±0.48 | 5.02 ±0.37 | 5.78 ±0.56 | 0.97 ±0.05 | 1.01 ±0.01 | 1.05 ±0.06 | 1.04 ±0.15 | 1.13 ±0.16 | 5.54 ±0.39 | 5.24 ±0.23 | 4.70 ±0.52 | 4.72 ±0.40 | 5.59 ±0.36 |
| | Bottom | 5.82 ±0.05 | 4.97 ±0.46 | 5.89 ±0.68 | 6.09 ±0.91 | 5.56 ±0.31 | 1.09 ±0.10 | 1.17 ±0.14 | 0.99 ±0.02 | 1.20 ±0.15 | 1.28 ±0.10 | 5.07 ±0.33 | 5.32 ±0.07 | 4.19 ±0.73 | 4.95 ±0.43 | 5.74 ±0.80 |

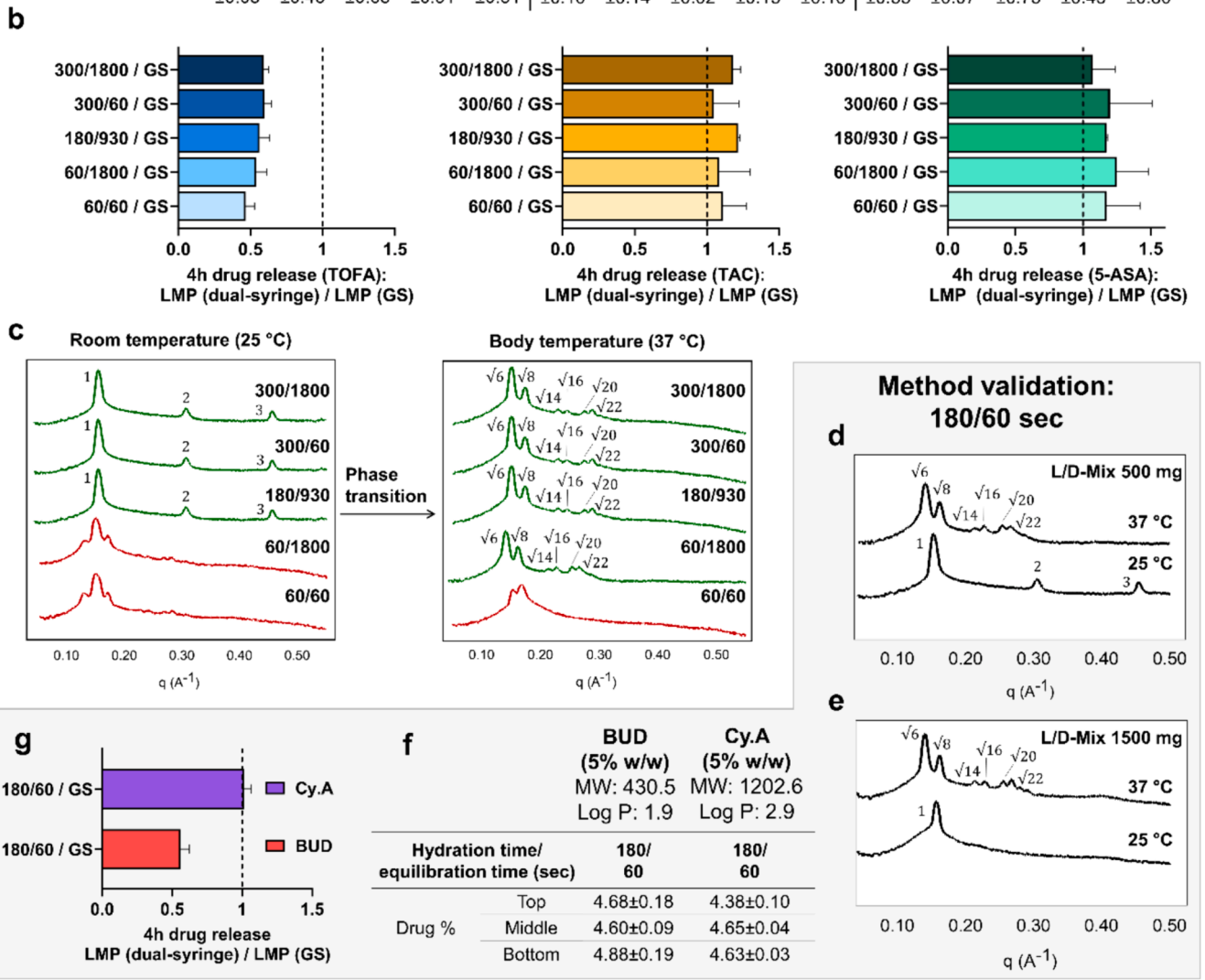


**f**

| | | BUD (5% w/w) MW: 430.5 Log P: 1.9 | Cy.A (5% w/w) MW: 1202.6 Log P: 2.9 |
|---|---|---|---|
| Hydration time/ equilibration time (sec) | | 180/ 60 | 180/ 60 |
| Drug % | Top | 4.68±0.18 | 4.38±0.10 |
| | Middle | 4.60±0.09 | 4.65±0.04 |
| | Bottom | 4.88±0.19 | 4.63±0.03 |

**Fig. 3.** Characterization of the five LMP produced by the dual-syringe method defined by DoE regarding (a) drug homogeneity (TOFA, TAC and 5-ASA) within the syringe, (b) 4 h drug release ratio of the LMP produced by the dual-syringe method and the LMP produced by the gold standard (GS) method (TOFA, TAC and 5-ASA), and (c) phase identity at 25 °C and 37 °C (LMP without drug). Validation of the optimal production method defined by DoE regarding phase identity at 25 °C and 37 °C with (d) 500 mg and (e) 1500 mg of L/D-Mix (LMP without drug), (f) drug homogeneity (BUD and Cy.A) within the syringe, and (g) 4 h drug release ratio of the LMP produced by the dual-syringe method and the LMP produced by the gold standard (GS) method (BUD and Cy.A). In panels a and f, MW: molecular weight (g/mol). In panels a, b, f and g, results are shown as mean ± SD (n = 2).

investigate whether LMP obtained by the proposed new method presents a lamellar phase at room temperature and an inverse bicontinuous cubic phase with Ia3d symmetry at body temperature. Interestingly, our findings demonstrate that the LMP structure is affected by the hydration time but not by the equilibration time (Fig. 3c). A minimum hydration time of 180 s is needed to obtain a lamellar phase (Lα) at 25 °C (green spectra), while the lowest hydration time (60 s) produces a less hydrated lamellar phase (Lc; red spectra). Provided that the minimum hydration time is performed, increasing the equilibration time from 60 to 1800 s does not impact the LMP phase.

Next, we validated the optimal hydration/equilibration times derived from the DoE: 180/60 s. Such a method provided the desired lamellar phase at 25 °C and a cubic gyroid at 37 °C with 500 mg or 1500 mg of formulation (Fig. 3d, e). Two other drugs (BUD and Cy.A) were incorporated into the mesophase and presented homogeneous drug distribution (Fig. 3f). Also, we compared the drug release profile from LMP produced by both methods (Fig. 3g), and we observed slower BUD release from the LMP produced by the dual-syringe method (as observed for LMP containing TOFA). On the other hand, Cy.A release was similar from the LMP produced by both methods; results that are comparable to

the ones observed for LMP containing TAC and 5-ASA. However, it is worth noting that the release media of LMP-Cy.A was enriched with ethanol to ensure drug solubility, and, in these circumstances, the drug release was partially driven by the gel erosion (100 % within 2 h, see Supplementary Fig. S5) [28].

Confocal Raman mapping was used as a complementary technique to ensure that a homogeneous drug distribution within the LMP (180/60 s) was obtained. The Raman spectra of pure Dimodan U/J and drug powders were initially collected and are shown in Supplementary Fig. S6. No significant differences in terms of drug homogeneity (TOFA, 5-ASA and BUD) were observed between LMP produced by the dual-syringe method (180/60 s) or by the gold standard method (Fig. 4). Unfortunately, it was not possible to clearly identify the signals of the drugs TAC and Cy.A in the LMP (Supplementary Fig. S7). Lastly, we confirmed by XRPD that the crystalline pattern of the lipid and drugs do not change after production of the LMP (Supplementary Fig. S8).

### 3.3. Predictive model for drug release

Experimental drug release data was used to train, test and validate a predictive model for small molecules drug release from LMP produced by the dual-syringe method. The data set used was composed of chemical descriptors of TOFA, TAC and 5-ASA, process parameters, and the amount of drug released from the LMP produced by the dual-syringe method at 1, 2, 3 and 4 h (Fig. 5a). We employed XGBoost regression, which is a gradient boosting algorithm widely used for regression tasks, employing decision trees as base learners to iteratively correct errors in predictions. It incorporates regularization techniques to prevent overfitting, optimization for performance, and offers a range of hyperparameters for tuning model performance, making it efficient, accurate, and scalable for handling complex datasets in various domains. The data set was split, of which 80 % was used for model training and optimization (Fig. 5b) and 20 % was used for testing the model (Fig. 5c). The accuracy of the predictive model is shown by the similar experimental and predicted drug release percentages and by the coefficient of determination ($r^2$ value) near 1. Further, the model's predictive power and accuracy were validated with a drug molecule (BUD) to which the model had no prior exposure, and the predictions were then compared to wet lab experiments (Fig. 5d). It is important to mention that the release of TOFA, TAC, 5-ASA, and BUD from the LMP is mainly driven by the diffusion of the drug through the mesophase water channels. Considering the enrichment of the release media of LMP-Cy.A with ethanol to ensure drug solubility and the consequent rapid drug release caused by the erosion of the LMP, we did not include Cy.A into the model.

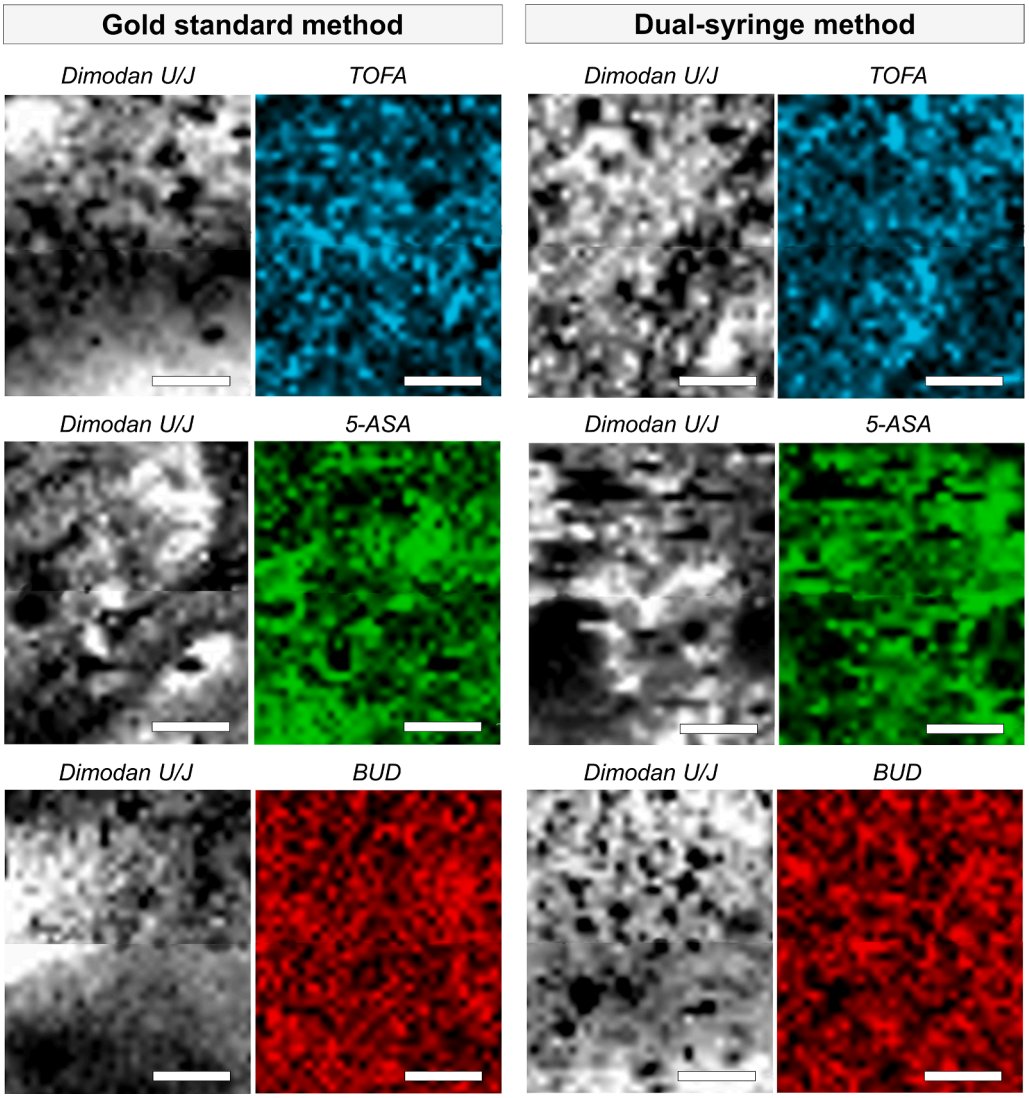


**Fig. 4.** Confocal Raman characterization of the LMP obtained by the gold standard method (first and second columns) and by the dual-syringe method (third and fourth columns). Two maps per sample were collected, imaging a total area of 1.6 mm × 2.0 mm. For the LMP containing TOFA (upper row), 5-ASA (middle row) and BUD (bottom row) it was possible to clearly distinguish the signals of the drug and the lipid within all the imaged area. The scale bars in each panel are 500 μ m.

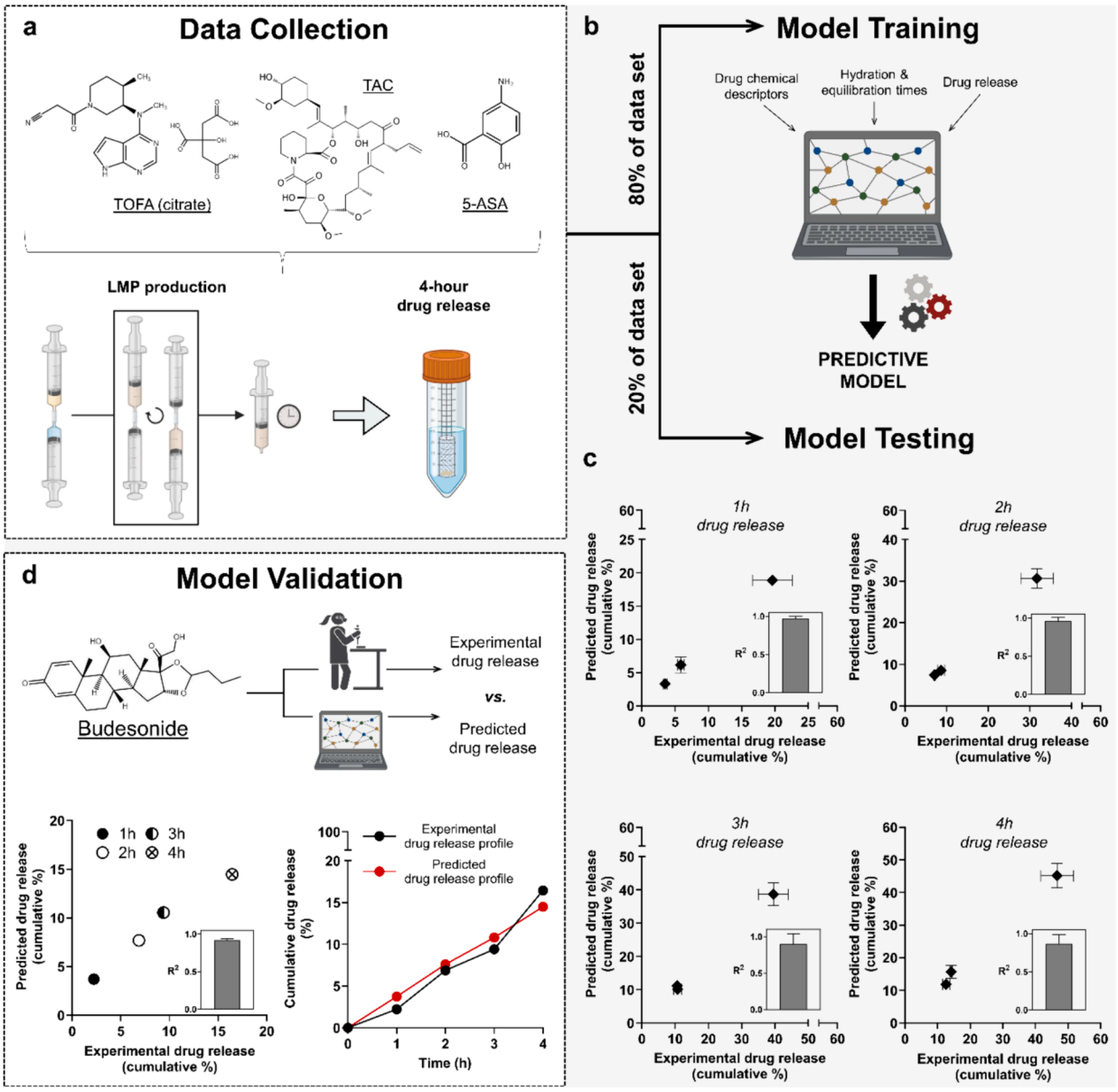


**Fig. 5.** Modelling approach for predicting drug release of small molecules from LMP produced by the dual-syringe method. (a) Data set composed of chemical descriptors of TOFA, TAC, and 5-ASA, process parameters and 4 h drug release profile from LMP produced by the dual-syringe method using the different hydration/equilibration times. (b) Model training and optimization with 80 % of the data set. (c) Model testing, with 20 % of the data set, for prediction of 1 h (top left), 2 h (top right), 3 h (bottom left) and 4 h (bottom right) drug release. Vertical error bars correspond to the standard deviation of the experimental drug release (n = 5) and horizontal error bars correspond to the standard deviation of the predicted drug release (n = 6). The bar plots show the $r^2$ derived by the model. (d) Model validation with BUD (n = 1). Predicted vs. experimental amount of drug released at each time point (left). Predicted and experimental 4 h release profile of BUD (right).

### *3.4. Rheological properties: Dual-syringe method vs. gold standard method*

While the TIF-Gel formulation screening and development was conducted using pure MLO as the lipid component [17], here we propose the use of an industrial food-grade monolinolein (Dimodan U/J), which brings the advantage of reduced cost and presents a waxy-solid consistency. To understand the impact of this variable on the rheological properties of the formulation, we prepared LMP by both methods using either MLO or Dimodan U/J. As shown in Fig. 6a, independently of the lipid and production method used, all gels exhibited shear-thinning flow behavior; however, when the dual-syringe method is applied, the viscosity increases, regardless of the type of lipid applied. Nevertheless, neither the total amount of drug released nor the drug release kinetics, which follows a Fickian diffusion profile modelled using the Higuchi equation, is highly affected by these variables (Fig. 6b). For the drug release investigation, we have chosen one drug model (5-ASA) to be incorporated into the LMP.

Next, applying Dimodan U/J as the lipid component, we investigated which parameters are responsible for the changes in viscosity; thus, we produced LMP by a modified gold standard method, in which no organic solvent (and thus no lyophilization) was used. Although all the formulations exhibited a shear-thinning behavior independently of the preparation method, the LMP obtained by the dual-syringe method and by the modified gold standard method presented higher flow points than the LMP obtained by the gold standard method, meaning that these gels have higher consistency at rest. Despite this, as the applied shear rate increases, the viscosity of the LMP produced by the modified gold standard method decreases to a greater extent than the LMP produced by the dual-syringe method (Fig. 6c). Therefore, amplitude sweep

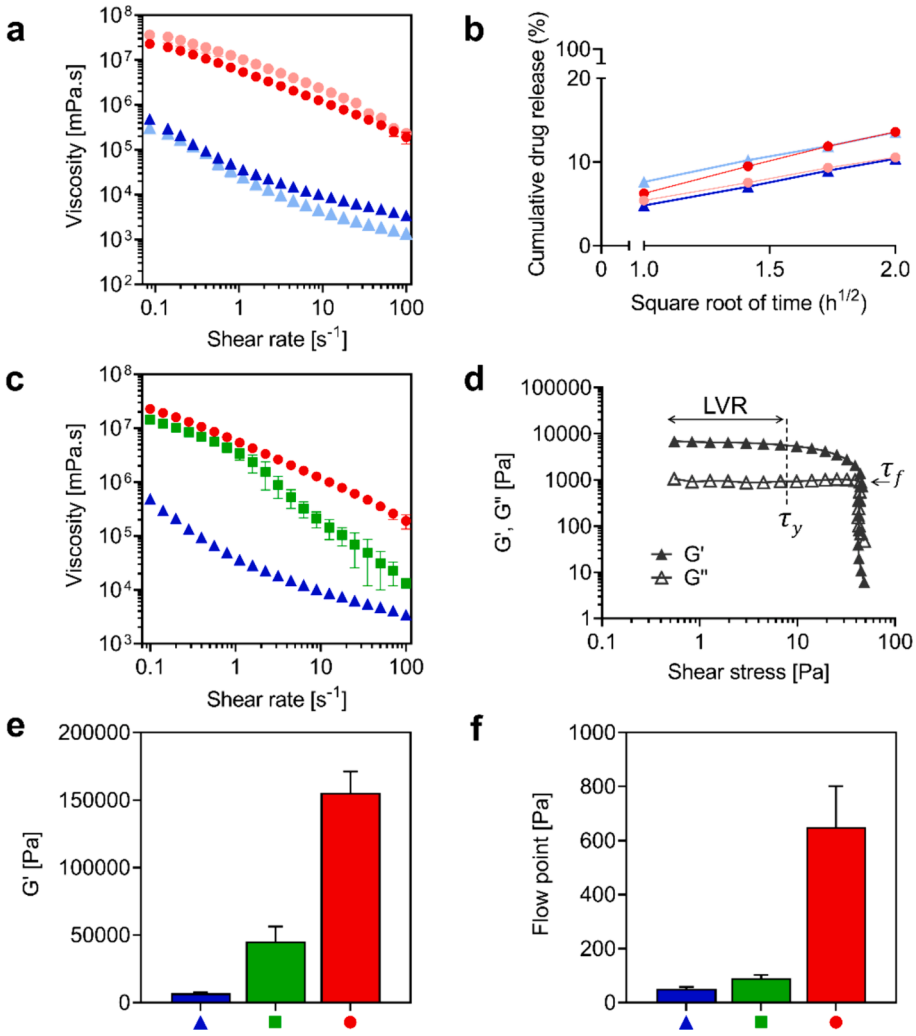


**Fig. 6.** Rheological characterization of LMP. (a) Viscosity vs. shear rate curve and (b) drug release vs. square root of time profile of LMP obtained by the gold standard method (triangles) composed of Dimodan U/J (dark blue) or MLO (light blue) and LMP obtained by the dual-syringe method (circles) composed of Dimodan U/J (red) or MLO (salmon). (c) Viscosity vs. shear rate curve of LMP obtained by the gold standard method (blue triangles), modified gold standard method (green squares) and dual-syringe method (red circles). (d) Representative amplitude sweep graph where the LVR and flow point ($\tau_f$) are indicated in the arrows, and LVR limit ($\tau_y$) is indicated in the dashed line. (e) G′ average in the LVR and (f) flow points of LMP produced with Dimodan (U/J) by the gold standard method (blue triangle), modified gold standard method (green square) or dual-syringe method (red circle). In panels a, c, e, and f, results are shown as mean ± SD (n = 3). (For interpretation of the references to colour in this figure legend, the reader is referred to the web version of this article.)

measurements were carried out to further investigate the viscoelastic features of the ensuing formulations by determining the yield points, the strength at rest, the linear viscoelastic region (LVR), and LVR limit ($\tau_y$) (Fig. 6d). Within this region, we observed storage modulus values (G′) higher than loss modulus values (G″) for the LMP produced by the three methods (Supplementary Fig. S9), meaning that the elastic components dominate regardless of the method of production used. However, in the LVR, G′ values of the LMP obtained by the dual-syringe method were nearly 23-fold and 3-fold higher than G′ values of the LMP obtained by the gold standard method and its modified version, respectively (Fig. 6e). This demonstrates that the dual-syringe method produces a lamellar phase with higher structural strength than the gold standard method, especially when organic solvents are employed. Besides that, the flow point ($\tau_f$, shear stress at G′ = G″) of LMP prepared by the dual-syringe method was nearly 13-fold and 7-fold higher than the $\tau_f$ of the LMP prepared by the gold standard method and its modified version, respectively (Fig. 6f), confirming that a higher shear needs to be applied for the lamellae to flow.

## 4. Discussion

### 4.1. Production of drug-loaded LMP

The translation of drug formulations from the laboratory to the industry scale often requires process adjustments and optimization to comply with pharmaceutical manufacturing regulations and ensure product quality. The application of the gold standard method is initially hindered by the use of organic solvents. Even though solvents with low toxic potential (Class 3) [29] could be applied for lipid and drug solubilization, for instance, ethanol and dimethyl sulfoxide, one should consider the large volumes needed for the industrial production of this formulation and possible short-term stability of the lipid and/or drug in solution. Besides that, the removal of the organic solvent, mainly obtained by lyophilization, must be efficient so that the residual amount of these chemicals is within the acceptable ranges [29]. The main reason for controlling the residual solvent amount is toxicity to the patient. Additionally, these substances, at certain levels, can induce drug phase

transformation and impact the physicochemical stability of the formulation [30]. The additional analytical steps and the environmental impact (i.e., increased chemical waste and energy consumption) that follow these steps are avoided in the dual-syringe method, providing a more sustainable and faster approach.

The next stages of LMP production include the incorporation of water into the lipid and drug mixture, and equilibration of the mesophase. In the gold standard method, the desired amount of formulation is hydrated and equilibrated altogether and, later, repartitioned into the primary packaging. To produce large batches, these two steps require optimization and careful monitoring. First, during the hydration step, the correct amount of water must be incorporated and homogenized throughout the mesophase, as slight changes in the water percentage could alter the mesophase structure. At lab scale this is guaranteed by mixing lipid and water with a spatula, together with several centrifugation steps, or by microliter syringes, however these procedures lack of scalability. Second, during the equilibration step, the system must be hermetically sealed to avoid moisture absorption and, thus, changes in the mesophase structure. Besides that, the end product must be sterilized by radiation since steam sterilization could alter the rheological properties of the LMP or its water content [31,32], and dry heat sterilization is not suitable for thermolabile drugs. These limitations are overcome by the dual-syringe method, in which a lipid-drug mixture (easily transferable into syringe A) is hydrated with WFI (contained in syringe B) just before application by the patient, and the desired phase identity is achieved within a minute, avoiding, also, the sterilization of the final gel.

Moreover, although the pure MLO is generally recognized as safe for human and/or animal use by the FDA [33], its counterpart Dimodan U/J has lower cost compared to the pure lipid, favoring its application in pharmaceutical and food sciences. Apart from scalability and cost reasons, while the pure MLO is in the liquid state at room temperature, Dimodan U/J is in a waxy but solid state. This property is favourable for the dual-syringe method because, once L/D-Mix is produced and the temperature and stirring are interrupted, the viscosity of the mixture gradually increases as it reaches room temperature. This characteristic improves L/D-Mix stability, especially for drugs with low affinity for the lipid (low Log P), as it prevents drug precipitation. In case pure MLO is applied, the mixture of lipid and drug (in the industrial container or in the individual syringes) should be maintained below 15 °C (MLO melting point) to avoid phase separation (Supplementary Fig. S10).

### 4.2. LMP production by the dual-syringe method

Our dual-syringe method proposes, as the first step, the production of L/D-Mix, which contains Dimodan U/J and drug. Homogeneous drug distribution was achieved by mixing L/D-Mix for 15 min. Lower mixing times, especially 5 min, were insufficient to properly homogenize the drug. For large-scale industrial production, additional studies are required to determine the optimal mixing time protocol based on batch size. Another important aspect to be considered when producing large batches is the storage conditions. Good manufacturing practices (GMP) require that the storage of starting materials, intermediate and bulk products should not impact their stability, safety, efficacy, or quality [34]. Therefore, hold-time studies are conducted to establish the time limits for holding these materials at different stages of production [34]. The stability of L/D-Mix was assessed in terms of drug precipitation, drug and lipid crystallinity, and drug degradation. The similar drug recovery values after 2 weeks of storage, even for the drugs with lower Log P (TOFA, 5-ASA and BUD), are likely related to the semisolid consistency of L/D-Mix, as increased viscosity can slow the drug diffusion rate [35]. L/D-Mix presented a similar crystallinity pattern at $t = 0$ and $t = 2$ weeks. However, we observed a slight increase in the degree of crystallinity of all the formulations, which is reasonable considering that upon storage the components could be able to self-assemble in a more ordered state [36].

Further, we have tested various hydration/equilibrations times, applying a DoE approach, to determine the optimal production conditions. Interestingly, the production of LMP by the dual-syringe method requires short hydration and equilibration times (180/60 s). We observed that hydrating the sample for only 60 s produced a lamellar phase (Lc) less hydrated than an Lα, since the hydration time is not sufficient to homogeneously distribute the water within the lipid matrix and parts of the gel present lower water content. Usually, LMP are equilibrated for several hours or days prior to use [5,8,15,17,18,37–41] while our findings demonstrate that a lamellar phase was achieved after 60 s of equilibration, highlighting the importance of hydration time over the equilibration time. We argue that the short equilibration time needed for producing this formulation is related to the incorporation of a low percentage of water (16 %) which results in a lamellar phase (Lα). The production of LMP in excess of water results in inverse hexagonal or cubic phases [5,8,15,18,23,37–39] and such mesophases might require a longer time to reach equilibrium. As confirmed by confocal Raman experiments, 180 s hydration time was also sufficient to distribute the drug within the LMP in a homogeneous manner. TAC and Cy.A signals could not be identified in the gel likely because the drugs signals almost completely overlap with those of the lipid, as shown in the spectra in Supplementary Fig. S6.

### 4.3. Drug release profile: Dual-syringe method vs. gold standard method

A correlation between hydration/equilibration times and drug release profile was not observed as, within each drug group, the values were similar. However, the drug release profile was influenced by the production method depending on the drug that is incorporated into the LMP. While LMP obtained by the gold standard method and by the dual-syringe method containing TAC, 5-ASA, and Cy.A presented similar drug release profiles, LMP obtained by the dual syringe method released TOFA and BUD slower in comparison to the gold standard method. The physicochemical properties of the drugs could be responsible for this phenomenon. The hydrophobic drug TAC (804.02 g/mol and Log P 3.2) presents a high affinity for the lipid phase together with a slow diffusion through the water channels, and, due to these characteristics, the production method did not influence the drug release. Cy.A also presents high molecular weight and Log P values (1202.61 g/mol and Log P 2.92); however, a rapid release was observed (100 % within 2 h for both production methods). This behaviour results from an erosion-driven drug release due to the enrichment of the release media with 30 % ethanol. The erosion of LMP-based beads by ethanol enriched media and its impact on drug release has been investigated by Allegritti and co-workers [28]. On the other hand, we have observed an influence of the production method on the drug release of TOFA and BUD, which present lower molecular weight and Log P values (504.50 g/mol and Log P 1.15 for TOFA, and 430.53 g/mol and Log P 1.9 for BUD). Possibly, the mechanical stirring of L/D-Mix (in the dual-syringe method) provides a more homogeneous and stable dispersion of the drug in the lipid matrix which ensures a slower drug release after hydration. Even though 5-ASA presents Log P value similar to TOFA (Log P 1.2), its smaller size (153.13 g/mol) allows for an easy diffusion through the water channels, and, in this case, the production method did not affect the release. The influence of drug hydrophilicity on the controlled release from LMP has been investigated by Martiel and co-workers [42]. Interestingly, their findings show that the release rate is not only affected by the partition coefficient, but also by the diffusion coefficient, which is influenced by the size or bulkiness of the drug molecule.

#### 4.3.1. Predictive model for drug release

Artificial intelligence (AI) based methods, including machine learning, have recently come into focus in the drug delivery field, paving the way for data-driven nanomedicine. Machine learning has the potential to predict properties and behaviour of drug delivery systems and can, thereby, be leveraged to streamline the experimental work [43,44].

Consequently, AI can significantly reduce the drug development workload, serving as a valuable tool in addition to the QbD approach [45]. In this paper, we have developed a predictive modelling approach for drug release of small molecules from LMP produced by the dual-syringe method. Our findings demonstrate the accuracy and effectiveness of the proposed predictive model, indicating its potential to facilitate the development of LMP-based delivery systems and the applicability of the dual-syringe method.

### *4.4. Rheological properties: Dual-syringe method vs. gold standard method*

Different viscous behaviour was observed between LMP produced by the two methods, independently of the lipid used (pure MLO vs. Dimodan U/J). We hypothesize that the use of organic solvents and possible residual amounts of these chemicals could explain the lower structural strength of LMP produced by the gold standard method. It has been reported that the type and concentration of organic solvent can affect the freezing characteristics of the solution [46]. Such characteristics, consequently, affect the freeze-drying process by modifications in the size and shape of ice crystals, drying rates, and reconstitution properties. Besides that, higher residual organic solvent levels have been associated with rapid freezing rates [47]. The influence of the organic solvent drying speed on the lattice size of cubic phases has been investigated by Kim and co-workers [48], and their findings suggest that super-swelled bicontinuous cubic single crystals, composed of a mixture of glycerol monooleate and polyethylene glycol in excess of water, are formed under fast drying conditions. However, to the best of our knowledge, the influence of organic solvents residues on LMP rheological characteristics has not been investigated.

## 5. Conclusion

In conclusion, we have developed a robust and scalable production method for drug-loaded LMP which may enable the transition of these drug delivery systems from lab-scale to industrial manufacturing. The industrial production of LMP by the standard method is hindered, mainly, by the use and subsequent removal of organic solvents [17,40], and the hydration and equilibration of large batches of gel. The proposed dual-syringe method, based on a QbD approach, avoids the use of organic solvents and, consequently, the lyophilization step. Moreover, the hydration and equilibration steps are better controlled as they occur in the syringe, and only before administration. Differently from the long equilibration times reported in the literature [17,39,41], our findings show that the equilibration of this mesophase is achieved within one minute. Our rheological measurements suggest that the new method produces LMP with higher structural strength than the gold standard method; nevertheless, further investigation is needed to better understand this phenomenon.

The versatility of this new production method was assessed by incorporating five drugs with diverse physicochemical properties, and, interestingly, we have observed that drugs with specific levels of hydrophobicity exhibit slower release from the mesophase when the dual-syringe method is applied. We have developed an accurate predictive model for the release of small molecules from LMP produced by the dual-syringe method.

Even though the proposed production method, combined with the predictive modelling approach, has the potential to facilitate and accelerate the advancement of LMP-based drug delivery systems, future work is needed to validate the dual-syringe method using LMP with diverse lipid compositions and water percentages, thereby consolidating its applicability.

## CRediT authorship contribution statement

**Rafaela Gazzi:** Writing – review & editing, Writing – original draft, Visualization, Validation, Methodology, Investigation, Formal analysis, Data curation, Conceptualization. **Rita Gelli:** Writing – review & editing, Writing – original draft, Methodology, Data curation, Conceptualization. **Remo Eugster:** Writing – review & editing, Methodology, Investigation, Data curation, Conceptualization. **Claudia Bühr:** Writing – review & editing, Methodology, Investigation. **Stefan Schürch:** Writing – review & editing, Data curation. **Raffaele Mezzenga:** Writing – review & editing, Data curation. **Paola Luciani:** Writing – review & editing, Supervision, Funding acquisition, Conceptualization. **Simone Aleandri:** Writing – review & editing, Writing – original draft, Visualization, Supervision, Data curation, Conceptualization.

## Declaration of competing interest

The authors declare the following financial interests/personal relationships which may be considered as potential competing interests: Aleandri Simone, Rafaela Gazzi and Paola Luciani have an International Patent Application pending (PCT/EP2023/076606). PL has received research funding from PPM Services SA. The other authors declare that they have no known competing financial interests or personal relationships that could have appeared to influence the work reported in this paper.

## Data availability

All data generated or analyzed during this study are included in this published article and its supplementary information file or are available from the corresponding author upon reasonable request. Source data are provided with this paper.

## Appendix A. Supplementary data

Supplementary data to this article can be found online at https://doi.org/10.1016/j.jcis.2024.09.099.

## References

[1] S. Hua, M.B.C. de Matos, J.M. Metselaar, G. Storm, Current trends and challenges in the clinical translation of nanoparticulate nanomedicines: pathways for translational development and commercialization, Front. Pharmacol. 9 (2018) 1–14, https://doi.org/10.3389/fphar.2018.00790.
[2] European Medicines Agency, "Quality by design." https://www.ema.europa.eu/en/human-regulatory-overview/research-and-development/quality-design (accessed Feb. 06, 2024).
[3] N.S. Mendonsa, A. Pradhan, P. Sharma, R.M.B. Prado, S.N. Murthy, S. Kundu, M. A. Repka, A quality by design approach to develop topical creams via hot-melt extrusion technology, Eur. J. Pharm. Sci. 136 (2019) 104948, https://doi.org/10.1016/j.ejps.2019.06.002.
[4] International Council for Harmonisation, "Pharmaceutical Development Q8(R2)," August. 2009.
[5] K.W.Y. Lee, T.-H. Nguyen, T. Hanley, B.J. Boyd, Nanostructure of liquid crystalline matrix determines in vitro sustained release and in vivo oral absorption kinetics for hydrophilic model drugs, Int. J. Pharm. 365 (2009) 190–199, https://doi.org/10.1016/j.ijpharm.2008.08.022.
[6] T.-H. Nguyen, T. Hanley, C.J.H. Porter, B.J. Boyd, Nanostructured liquid crystalline particles provide long duration sustained-release effect for a poorly water soluble drug after oral administration, J. Control. Release 153 (2011) 180–186, https://doi.org/10.1016/j.jconrel.2011.03.033.
[7] R. Saklani, P.K. Yadav, M.A. Nengroo, S.L. Gawali, P.A. Hassan, D. Datta, D. P. Mishra, I. Dierking, M.K. Chourasia, An injectable in situ depot-forming lipidic lyotropic liquid crystal system for localized intratumoral drug delivery, Mol. Pharm. 19 (2022) 831–842, https://doi.org/10.1021/acs.molpharmaceut.1c00782.
[8] B.J. Boyd, D.V. Whittaker, S.-M. Khoo, G. Davey, Lyotropic liquid crystalline phases formed from glycerate surfactants as sustained release drug delivery systems, Int. J. Pharm. 309 (2006) 218–226, https://doi.org/10.1016/j.ijpharm.2005.11.033.

[9] B.J. Boyd, D.V. Whittaker, S.-M. Khoo, G. Davey, Hexosomes formed from glycerate surfactants-Formulation as a colloidal carrier for irinotecan, Int. J. Pharm. 318 (2006) 154–162, https://doi.org/10.1016/j.ijpharm.2006.03.010.
[10] B.J. Boyd, S.-M. Khoo, D.V. Whittaker, G. Davey, C.J.H. Porter, A lipid-based liquid crystalline matrix that provides sustained release and enhanced oral bioavailability for a model poorly water soluble drug in rats, Int. J. Pharm. 340 (2007) 52–60, https://doi.org/10.1016/j.ijpharm.2007.03.020.
[11] M.H. Ki, J.L. Lim, J.K. Ko, S.H. Park, J.E. Kim, H.J. Cho, E.S. Park, D.D. Kim, A new injectable liquid crystal system for one month delivery of leuprolide, J. Control. Release 185 (2014) 62–70, https://doi.org/10.1016/j.jconrel.2014.04.034.
[12] L.B. Lopes, D.A. Ferreira, D. de Paula, M.T.J. Garcia, J.A. Thomazini, M.C. A. Fantini, M.V.L.B. Bentley, Reverse hexagonal phase nanodispersion of monoolein and oleic acid for topical delivery of peptides: in vitro and in vivo skin penetration of cyclosporin, Pharm. Res. 23 (6) (2006) 1332–1342, https://doi.org/10.1007/s11095-006-0143-7.
[13] N.K. Swarnakar, V. Jain, V. Dubey, D. Mishra, N.K. Jain, Enhanced oromucosal delivery of progesterone via hexosomes, Pharm. Res. 24 (12) (2007) 2223–2230, https://doi.org/10.1007/s11095-007-9409-y.
[14] C. Leal, N.F. Bouxsein, K.K. Ewert, C.R. Safinya, Highly efficient gene silencing activity of siRNA embedded in a nanostructured gyroid cubic lipid matrix, J. Am. Chem. Soc. 132 (2010) 16841–16847, https://doi.org/10.1021/ja1059763.
[15] S. Kozaka, R. Wakabayashi, N. Kamiya, M. Goto, Design of swollen lipidic cubic phase to increase transcutaneous penetration of biomacromolecules, ACS Appl. Mater. Interfaces 13 (2021) 54753–54761, https://doi.org/10.1021/acsami.1c16659.
[16] R. Mezzenga, C. Meyer, C. Servais, A.I. Romoscanu, L. Sagalowicz, R.C. Hayward, Shear rheology of lyotropic liquid crystals: a case study, Langmuir 21 (2005) 3322–3333, https://doi.org/10.1021/la046964b.
[17] M. Carone, M.R. Spalinger, R.A. Gaultney, R. Mezzenga, A. Mookhoek, P. Krebs, G. Rogler, P. Luciani, S. Aleandri, Temperature-triggered in situ forming lipid mesophase gel for local treatment of ulcerative colitis, Nat. Commun. 14 (2023) 3489, https://doi.org/10.1038/s41467-023-39013-3.
[18] W.-K. Fong, T. Hanley, B.J. Boyd, Stimuli responsive liquid crystals provide 'on-demand' drug delivery in vitro and in vivo, J. Control. Release 135 (2009) 218–226, https://doi.org/10.1016/j.jconrel.2009.01.009.
[19] S. Aleandri, R. Mezzenga, The physics of lipidic mesophase delivery systems, Phys. Today 73 (7) (2020) 38–44, https://doi.org/10.1063/PT.3.4522.
[20] Camurus, "Buvidal prolonged-release solution for injection." https://www.camurus.com/science/products/.
[21] F. Blachier, Alimentation, bacterial metabolites, and host intestinal epithelium, in: Metabolism of Alimentary Compounds by the Intestinal Microbiota and Health, 2023, pp. 145–188.
[22] C. Edmonds, Absorption and secretion of fluid and electrolytes by the rectum, Scand. J. Gastroenterol. 93 (1984) 79–87.
[23] Y. Yao, S. Catalini, P. Foggi, R. Mezzenga, Water-lipid interface in lipidic mesophases with excess water, Faraday Discuss. 249 (2023) 469–484, https://doi.org/10.1039/d3fd00118k.
[24] L.X. Yu, Pharmaceutical quality by design: product and process development, understanding, and control, Pharm. Res. 25 (4) (2008) 781–791, https://doi.org/10.1007/s11095-007-9511-1.
[25] A.S. Rathore, H. Winkle, Quality-by-design approach for biopharmaceuticals, Nat. Biotechnol. 27 (1) (2009) 26–34, https://doi.org/10.1038/nbt0109-26.
[26] M. Caffrey, V. Cherezov, Crystallizing membrane proteins using lipidic mesophases, Nat. Protoc. 4 (5) (2009) 706–731, https://doi.org/10.1038/nprot.2009.31.
[27] V. Karavelidis, E. Karavas, D. Giliopoulos, S. Papadimitriou, D. Bikiaris, Evaluating the effects of crystallinity in new biocompatible polyester nanocarriers on drug release behavior, Int. J. Nanomed. 6 (2011) 3021–3032, https://doi.org/10.2147/ijn.s26016.
[28] E. Allegritti, L. Giansanti, G. Bordon, M.A. Maggi, P. Luciani, S. Aleandri, Unlocking new dimensions in long-acting injectables using lipid mesophase-based beads, J. Colloid Interface Sci. 664 (2024) 1031–1041, https://doi.org/10.1016/j.jcis.2024.03.067.
[29] International Council for Harmonisation, Impurities: Guideline for Residual Solvents Q3C(R8), April. 2021.
[30] K. Grodowska, A. Parczewski, Organic solvents in the pharmaceutical industry, Acta Pol. Pharm. – Drug Res. 67 (1) (2010) 3–12.
[31] R. Galante, T.J.A. Pinto, R. Colaço, A.P. Serro, Sterilization of hydrogels for biomedical applications: a review, J. Biomed. Mater. Res. Part B 106B (2018) 2472–2492, https://doi.org/10.1002/jbm.b.34048.
[32] W.L. Stoppel, J.C. White, S.D. Horava, A.C. Henry, S.C. Roberts, S.R. Bhatia, Terminal sterilization of alginate hydrogels: efficacy and impact on mechanical properties, J. Biomed. Mater. Res. Part B 102B (2014) 877–884, https://doi.org/10.1002/jbm.b.33070.
[33] *21 C.F.R § 184.1505*, 2023.
[34] World Health Organisation, Annex 4 - General guidance on hold-time studies, WHO Tech. Rep. Ser. 992 (2015) 87–93.
[35] S. Xua, W.G. Dai, Drug precipitation inhibitors in supersaturable formulations, Int. J. Pharm. 453 (1) (2013) 36–43, https://doi.org/10.1016/j.ijpharm.2013.05.013.
[36] R.H. Müller, M. Radtke, S.A. Wissing, Solid lipid nanoparticles (SLN) and nanostructured lipid carriers (NLC) in cosmetic and dermatological preparations, Adv. Drug Deliv. Rev. 54 (Suppl) (2002) 131–155, https://doi.org/10.1016/S0169-409X(02)00118-7.
[37] Y.-D. Dong, I. Larson, T. Hanley, B.J. Boyd, Bulk and dispersed aqueous phase behavior of phytantriol: effect of vitamin E acetate and F127 polymer on liquid crystal nanostructure, Langmuir 22 (2006) 9512–9518, https://doi.org/10.1021/la061706v.
[38] R. Negrini, R. Mezzenga, Diffusion, molecular separation, and drug delivery from lipid mesophases with tunable water channels, Langmuir 28 (2012) 16455–16462, https://doi.org/10.1021/la303833s.
[39] Q.-Q. Shan, X.-J. Jiang, F.-Y. Wang, Z.-X. Shu, G. Shuang-Ying, Cubic and hexagonal liquid crystals as drug carriers for the transdermal delivery of triptolide, Drug Deliv. 26 (1) (2019) 490–498, https://doi.org/10.1080/10717544.2019.1602796.
[40] M. Carone, R. Gazzi, R. Eugster, R. Gelli, N. Manten, A.A. Ganguin, S. Di Valerio, G. Yadav, P. Castaldo, R. Mezzenga, P. Luciani, S. Aleandri, 3D-printed lipid mesophases for the treatment of chronic liver disease, Adv. Mater. Technol. (2024) 2301930, https://doi.org/10.1002/admt.202301930.
[41] T.G. Meikle, D.W. Keizer, J.J. Babon, C.J. Drummond, F. Separovic, C.E. Conn, S. Yao, Physiochemical characterization and stability of lipidic cubic phases by solution NMR, Langmuir 36 (2020) 6254–6260, https://doi.org/10.1021/acs.langmuir.0c00949.
[42] I. Martiel, N. Baumann, J.J. Vallooran, J. Bergfreund, L. Sagalowicz, R. Mezzenga, Oil and drug control the release rate from lyotropic liquid crystals, J. Control. Release 204 (2015) 78–84, https://doi.org/10.1016/j.jconrel.2015.02.034.
[43] S. Rezvantalab, S. Mihandoost, M. Rezaiee, Machine learning assisted exploration of the influential parameters on the PLGA nanoparticles, Sci. Rep. 14 (2024) 1114, https://doi.org/10.1038/s41598-023-50876-w.
[44] P. Bannigan, Z. Bao, R.J. Hickman, M. Aldeghi, F. Häse, A. Aspuru-Guzik, C. Allen, Machine learning models to accelerate the design of polymeric long-acting injectables, Nat. Commun. 14 (2023) 35, https://doi.org/10.1038/s41467-022-35343-w.
[45] M.H.S. Dawoud, I.S. Mannaa, A. Abdel-Daim, N.M. Sweed, Integrating artificial intelligence with quality by design in the formulation of lecithin/chitosan nanoparticles of a poorly water - soluble drug, AAPS PharmSciTech 24 (2023) 169, https://doi.org/10.1208/s12249-023-02609-5.
[46] D.L. Teagarden, D.S. Baker, Practical aspects of lyophilization using non-aqueous co-solvent systems, Eur. J. Pharm. Sci. 15 (2002) 115–133, https://doi.org/10.1016/S0928-0987(01)00221-4.
[47] C. Kunz, H. Gieseler, Factors influencing the retention of organic solvents in products freeze-dried from co-solvent systems, J. Pharm. Sci. 107 (2018) 2005–2012, https://doi.org/10.1016/j.xphs.2018.04.001.
[48] H. Kim, Z. Song, C. Leal, Super-swelled lyotropic single crystals, Proc. Natl. Acad. Sci. 114 (41) (2017) 10834–10839, https://doi.org/10.1073/pnas.1710774114.